Available online at www.sciencedirect.com
ScienceDirect
Tetrahedron 63 (2007) 11902–11910
Tetrahedron

Computational and experimental studies of the conformational reactions of 1,3,5-tris(pentaphenylphenyl)benzene

Robert A. Pascal, Jr.,[a,*] Christina M. Kraml,[b] Neal Byrne[b] and Frederick J. Coughlin[a]

[a]*Department of Chemistry, Princeton University, Princeton, NJ 08544, USA*
[b]*Lotus Separations, Princeton, NJ 08544, USA*

Received 31 July 2007; revised 11 September 2007; accepted 12 September 2007
Available online 15 September 2007

Abstract—Computational analyses of the five possible functional group rotations in 1,3,5-tris(pentaphenylphenyl)benzene (**1**) were conducted at three disparate levels of theory: AM1, HF/STO-3G, and B3LYP/6-31G(d). The ground state and transition state structures were located for all of the conformational reactions, and the free energies of activation for these processes were calculated. In addition, compound **1** was resolved by low-temperature chromatography on a chiral support, and its barrier to racemization was determined by dynamic chromatography. These computational and experimental results are compared with data from dynamic NMR studies of **1** in the literature.

1. Introduction

The synthesis and structural characterization of 'polyphenylene nanostructures' have been a major research enterprise in recent years.[1] In the design and evaluation of these structures, chemical notions of molecular 'rigidity' and 'flexibility' are frequently invoked, but there have been relatively few investigations, either experimental or computational, of the dynamic properties of these large molecules.[2–4] Because of their size, the experimental spectra of polyphenylenes are usually complex, and computational work at even moderate levels of theory is quite onerous. Both factors have discouraged detailed studies of the dynamic properties of complex polyphenylenes. In addition, even where experimental and computational studies exist for the same molecule, it is no simple matter to compare the results in a meaningful way.

For this reason the work of Komber and co-workers,[3,4] who have used dynamic NMR spectroscopy to study functional group rotations and other conformational processes in a variety of highly branched polyphenylenes, is particularly important. Because the solution NMR spectra can be unambiguously assigned, the identity of the conformational process under examination is certain. One of the molecules that they investigated—1,3,5-tris(pentaphenylphenyl)benzene (**1**, Scheme 1)—is especially well suited for the comparison of theory with experiment. This is one of the first polyphenylene dendrimers to have been prepared and crystallographically characterized.[5] It is a fairly large molecule ($C_{114}H_{78}$), but, because of its high symmetry (D_3), its proton and carbon NMR spectra are reasonably simple, and the number of distinct functional group rotations in this molecule is small.

Compound **1** is a chiral molecule, a molecular propeller, and both enantiomers are illustrated in Scheme 1. There are five processes that involve rotations about arene–arene bonds in **1**. The simplest are the rotations of the three chemically inequivalent phenyl rings A, B, and C about bonds *a*, *b*, and *c*, respectively. A fourth process is a 180° rotation of one of the pentaphenylphenyl 'blades' about bond *d*. The fifth, perhaps less obvious process is the concerted 60° rotation of all three blades that interconverts the two enantiomers of compound **1**.

By good fortune, experimental data exist that bear on the free energies of activation ($\Delta G^{\ddagger}$) for at least three of these five processes. In Tong et al.'s original paper describing the synthesis of **1**, the barrier to 180° blade rotation was determined to be 18.9 kcal/mol by variable temperature (VT) proton NMR studies of a hexamethoxy derivative of **1**.[5] Komber et al., also using VT proton NMR, measured the barriers for the rotations of rings A and B to be 16.9 and 18.0 kcal/mol, respectively.[4] In addition, Tong et al. recorded the carbon NMR spectrum of **1** at room temperature and observed only 18 lines, the number expected for rapid phenyl rotation or rapid enantiomerization (or both) in compound **1**.[5] However, when Komber et al. recorded the same spectrum at

Keywords: Polyphenylenes; Oligophenylenes; Conformational analysis; Transition state analysis; Chromatographic resolution.
* Corresponding author. Tel.: +1 609 258 5417; fax: +1 609 258 6746; e-mail: snake@chemvax.princeton.edu

0040–4020/$ - see front matter © 2007 Elsevier Ltd. All rights reserved.
doi:10.1016/j.tet.2007.09.021

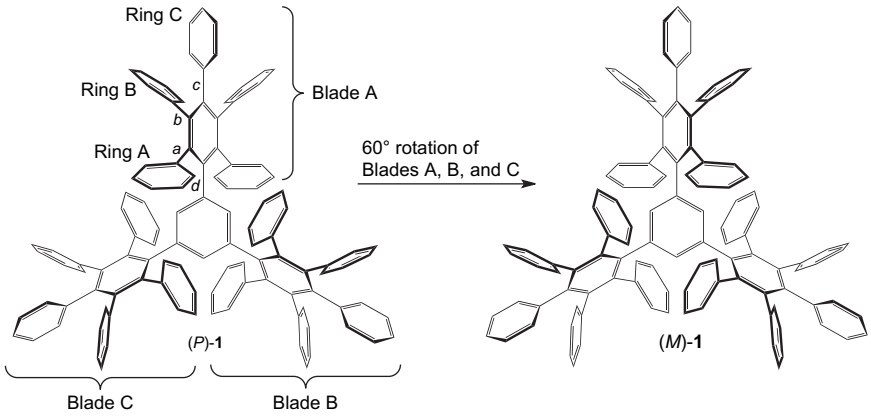

Scheme 1.

higher field (125.2 MHz vs 67.9 MHz for Tong et al.), they resolved three pairs of closely spaced lines, yielding a total of 21 observed resonances.[3] This result might reflect either slow phenyl rotation in **1** or slow interconversion of the enantiomers.

How well do modern computational methods describe the conformational reactions of a complex molecule such as compound **1**? Computational packages such as Gaussian 03[6] contain powerful algorithms for finding and characterizing transition state (TS) structures in such reactions, and the difference in the calculated energies of the transition state and the ground state structures can be compared directly to the experimental $\Delta G^{\ddagger}$'s for these processes. In this paper we report computational analyses of the five conformational reactions of compound **1** at three very different levels of theory: semiempirical molecular orbital calculations (AM1[7]), low-level Hartree–Fock calculations (HF/STO-3G[8]), and the common hybrid density functional method B3LYP/6-31G(d).[9,10] In addition, we report the experimental resolution of compound **1** into its enantiomers and provide an estimate for the barrier to racemization ($\Delta G^{\ddagger}_{rac}$). The results of the calculations and new and existing experimental data are compared with the hope that a reasonable level of theory may be chosen for future studies of the conformational dynamics of large polyphenylenes. In addition, for pedagogical purposes, we have described as carefully as possible the process by which the various computational minima and saddle points were located and characterized for this unusually large molecule.

2. Results

2.1. The ground state structure of compound 1 and the effect of symmetry on transition state analysis

Both crystallographically independent molecules in the X-ray structure of 1,3,5-tris(pentaphenylphenyl)benzene (**1**) are molecular propellers that possess approximate D_3 symmetry,[5] and preliminary studies using molecular mechanics (Sybyl,[11] MMFF[12]), semiempirical (AM1[7]), ab initio (HF/STO-3G, HF/3-21G[8]), and density functional [B3LYP/6-31G(d)[9,10]] calculations all indicated that the likely ground state conformation of compound **1** possesses exact D_3 symmetry. There are, of course, two enantiomers of this D_3 conformation. Only at the HF/STO-3G level has any other potential minimum been located, a C_{3h}-symmetric structure to be discussed shortly.

The presence of only two, enantiomeric potential minima in a molecule of relatively high symmetry is a favorable situation for the computational analysis of its conformational reactions. First, any one-dimensional TS (a saddle point of order 1) that is located computationally for compound **1** must characterize either (1) a degenerate functional group rotation (in the absence of labels) that links two molecular propellers of the same chirality or (2) a conformational process that interconverts the two enantiomers (an 'enantiomerization' or racemization reaction). Second, it is quite possible that the TS structures for some of the conformational interconversions will themselves possess a symmetry element, and this will greatly simplify the search for the transition states. In addition, any TS that contains a mirror plane necessarily connects the two enantiomers and represents a pathway for the racemization of compound **1**.

Computational geometry optimizations that employ symmetry constraints require vastly less time than unconstrained optimizations. Analytical frequency calculations can then be used to characterize these symmetric structures as potential minima, one-dimensional transition states, or higher order saddle points, and these calculations also require much less time when symmetry is present. Optimizations of the geometry of compound **1** under the constraint of D_3 symmetry at the AM1, HF/STO-3G, and B3LYP/6-31G(d) levels yield propeller-shaped structures that strongly resemble the X-ray crystal structure of **1**. Frequency calculations at all three levels indicate that these structures are potential minima (the frequency calculations yield zero imaginary normal modes for each, as indicated in Table 1). A stereoview of the B3LYP/6-31G(d)-optimized structure of D_3-**1** is illustrated in Figure 1. The energies of these structures (including the zero-point energy corrections obtained from the frequency calculations) are taken to be the ground state energies of compound **1** at their respective levels of theory. In this paper, the zero-point corrected relative energies [$\Delta(E$+ZPE)] of the calculated structures are found in Table 1, as well as the calculated relative free energies [ΔG_{298}] for comparison with the experimental $\Delta G^{\ddagger}$'s, where available.

Table 1. Calculated energies for conformations and conformational transition states of 1,3,5-tris(pentaphenylphenyl)benzene (**1**) at three levels of theory

Conformation	Symmetry	AM1			HF/STO-3G			B3LYP/6-31G(d)				Exptl $\Delta G^{\ddagger}$ (T)
		ΔE_{corr}	ΔG_{298}	n_I	ΔE_{corr}	ΔG_{298}	n_I	ΔE_{corr}	ΔG_{298}	n_I	ν_{min}	
Ground state (**1**)	D_3	0.0	0.0	[0]	0.0	0.0	[0]	0.0	0.0	[0]	{+7.5}	0.0
Triple 60° blade rotation TS	D_{3h}	26.4	37.3	[8]	31.8	40.7	[8]	33.4	41.0	[8]	{−45.0}	
Triple 60° blade rotation TS	C_{3h}	17.8	18.9	[1]	26.3[a]	23.6	[0]	22.8	20.8	[1]	{−12.8}	20.8 (288 K)[d,e]
180° Blade rotation TS	C_{2v}	21.5	26.7	[2]	28.7	29.7	[2]	28.8	31.0	[4]	{−19.5}	
180° blade rotation TS	C_s	20.0	21.5	[1]	28.7	27.2	[1]	26.5	26.8	[2]	{−16.9}	
180° blade rotation TS	C_1	[b]			[b]			24.6	25.4	[1]	{−11.7}	18.9 (333 K)[f]
Ring A rotation TS	C_1	16.0	16.7	[1]	25.6	25.8	[1]	19.1	19.9	[1]	{−53.7}	16.9 (352 K)[g]
Ring B rotation TS	C_1	16.3	19.0	[1]	25.7	26.3	[1]	19.8	20.2	[1]	{−79.8}	18.0 (374 K)[g]
Ring C rotation TS	C_2	18.0	22.5	[2]	24.4	24.1	[1]	21.1	24.5	[2]	{−98.0}	
Ring C rotation TS	C_1	16.7	19.1	[1]	[c]			19.8	20.8	[1]	{−79.2}	

For each entry, the zero-point corrected relative energy [ΔE_{corr}=Δ(E+ZPE), kcal/mol] is given, followed by the relative free energy [ΔG_{298}], and the number of imaginary frequencies [n_I] in brackets (the calculated absolute energies (E), zero-point corrected energies (E+ZPE), and free energies (G_{298}) are found in the Supplementary data.). For the B3LYP stationary points, the lowest calculated frequency (ν_{min}, cm^{-1}) is given in braces. The experimental free energies of activation for the rotations corresponding to the calculated transition states, where known, are given in the last column.

[a] No TS has been located connecting the D_3 and C_{3h} minima at the HF/STO-3G level.

[b] Not applicable; the TS structure has C_s symmetry at this level.

[c] Not applicable; the TS structure has C_2 symmetry at this level.

[d] This work.

[e] This experimental $\Delta G^{\ddagger}$ may correspond to the 60° rotation, the 180° rotation, or a combination of both (see text).

[f] Ref. 5.

[g] Ref. 4.

With the likely ground state of compound **1** properly characterized, the next step is to identify which of the five rotations depicted in Scheme 1 might proceed through symmetric transition states. It is clear that the TS structures for the rotations of rings A and B (about bonds *a* and *b*, respectively) are unlikely to possess any symmetry. However, the bonds *c* and *d* lie on C_2 axes in compound **1**, and thus the conformational interconversions that involve rotations about these bonds (the ring C rotations and the pentaphenylphenyl blade rotations, respectively) might possess symmetric TS structures. Once the symmetric stationary points have been characterized, the more onerous task of locating the asymmetric transition states will be undertaken.

2.2. The triple 60° blade rotation transition state

Of the processes identified in Scheme 1, the triple 60° blade rotation TS is the only one that might retain the C_3 axis of compound **1**. Indeed, one can imagine a TS for this process in which all three blades are perpendicular to the central ring in a D_{3h}-symmetric structure. (D_{3h} is the highest symmetry that compound **1** may attain.) However, geometry optimizations for compound **1** under the constraint of D_{3h} symmetry at the AM1, HF/STO-3G, and B3LYP/6-31G(d) levels of theory, followed by frequency calculations, indicate that D_{3h}-**1** is a saddle point of order 8 (!) at all three levels (Table 1). Therefore, such a structure is chemically irrelevant.

How else might a triple blade rotation proceed? A high-symmetry alternative would be to bend the 'tops' of all three propeller blades in the same direction to yield a C_3- or C_{3h}-symmetric structure that would evolve into the enantiomeric propeller by the subsequent bending of the 'bottoms' of the blades in the opposite direction. Such a process is shown schematically in Scheme 2. It was therefore pleasing to find that geometry optimization of compound **1** under the constraint of C_{3h} symmetry, followed by frequency calculations, showed that C_{3h}-**1** is indeed an important structure for the racemization of compound **1**. At the AM1 and B3LYP/6-31G(d) levels there is only one imaginary frequency, and animation of the imaginary normal mode indicates that C_{3h}-**1** is a plausible TS for the triple blade rotation. Furthermore, any slight distortion of the structure that breaks the mirror plane, followed by geometry optimization, results in one or the other enantiomer of D_3-**1**, as expected for a genuine TS. A stereoview of the B3LYP/6-31G(d)-optimized structure of C_{3h}-**1** is illustrated in Figure 1.

The calculated free energies of C_{3h}-**1** at the AM1 and B3LYP/6-31G(d) levels are 18.9 and 20.8 kcal/mol, respectively, above those of D_3-**1** (see Table 1); thus these are estimates of $\Delta G^{\ddagger}$ for the enantiomerization of compound **1**. If true, then the half-life for the racemization should be at most a few minutes at room temperature. As will be seen from an experimental study described later, this is an excellent estimate.

Interestingly, at the HF/STO-3G level C_{3h}-**1** is a potential minimum, not a transition state, and it is the only other potential minimum located for compound **1** at any level of theory. Despite a great deal of effort, no TS was found that linked the D_3 and C_{3h} minima at the HF/STO-3G level. However, the calculated free energy of this intermediate is 23.6 kcal/mol above the ground state, and this places a lower limit on the $\Delta G^{\ddagger}_{rac}$ that is rather higher than those calculated at the AM1 and B3LYP/6-31G(d) levels.

2.3. The 180° blade rotation transition state

The rotation of a single blade about bond *d* cannot have a TS structure that retains the C_3 axis of compound **1**. The highest

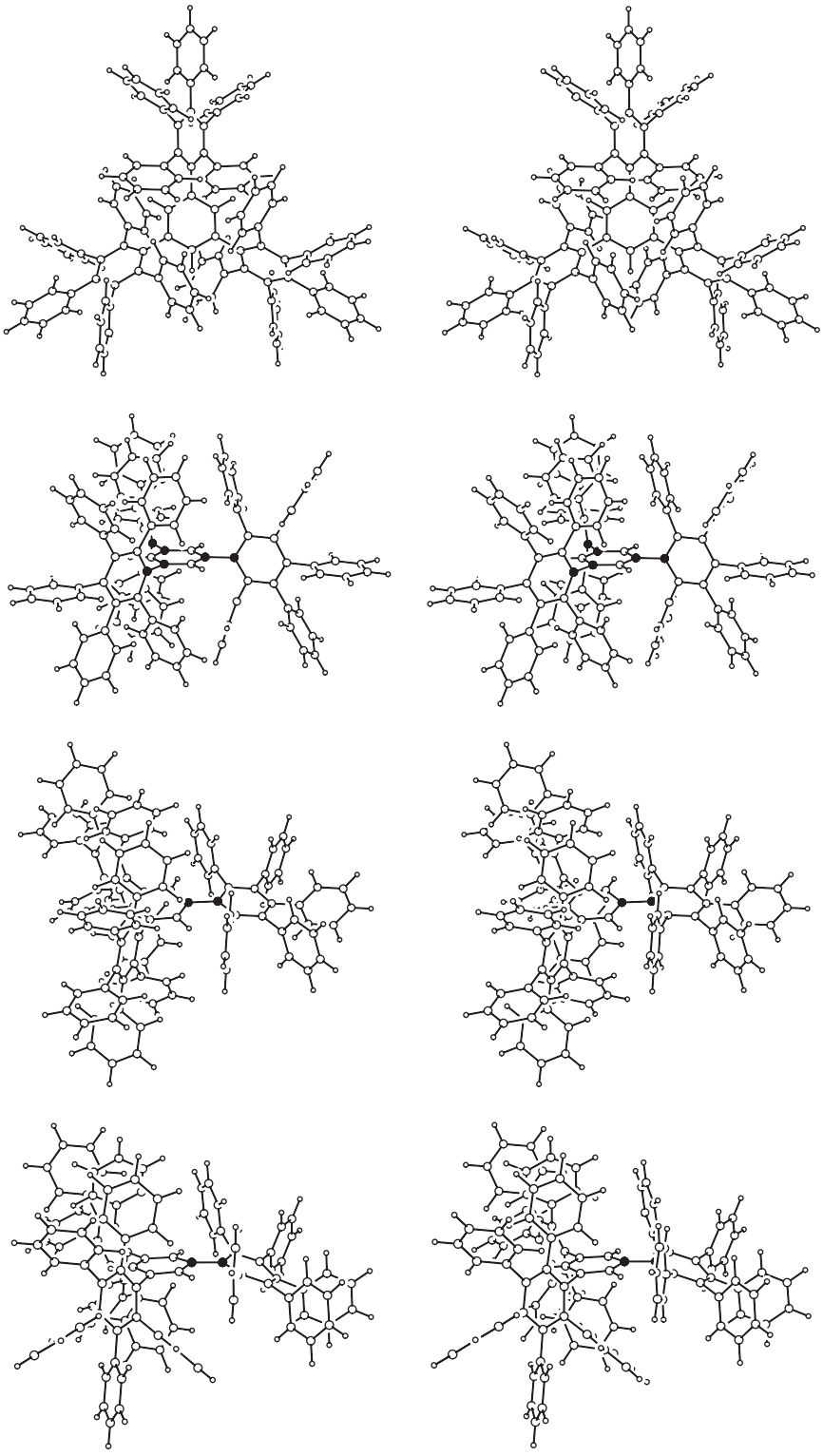

Figure 1. Stereoviews of calculated stationary point structures for compound **1**. Top to bottom: the B3LYP/6-31G(d) ground state (D_3), the B3LYP/6-31G(d) triple 60° blade rotation TS (C_{3h}), the HF/STO-3G 180° blade rotation TS (C_s), and the B3LYP/6-31G(d) 180° blade rotation TS (C_1). The solid black spheres are the carbon atoms around which the principal bond rotations occur.

symmetry that such a TS may possess is C_{2v}, where two of the blades are perpendicular to the central ring and the third, rotating blade is parallel. Geometry optimizations of such a structure at the usual levels under the constraint of C_{2v} symmetry, followed by frequency calculations, indicated that C_{2v}-**1** is a saddle point of order 2 at the AM1 and HF/STO-3G levels, and a saddle point of order 4 at the B3LYP/6-31G(d) level (Table 1). The simpler situation at the lower two levels of theory will be analyzed first.

Animation of the imaginary normal modes of C_{2v}-**1** at the AM1 and HF/STO-3G levels showed that the mode not

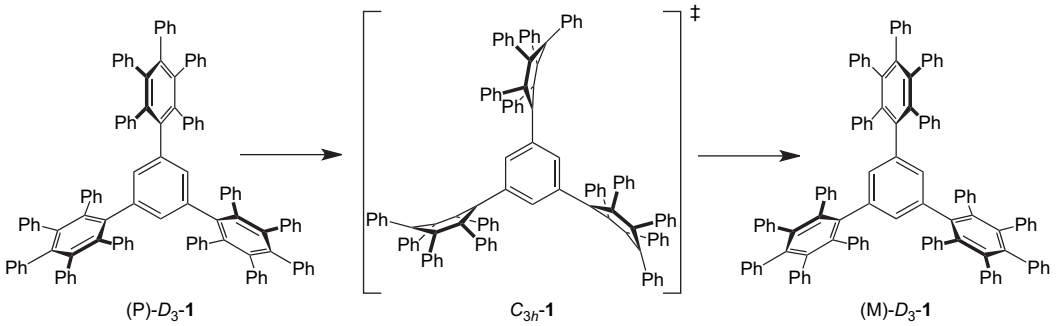

Scheme 2.

corresponding to the blade rotation was a distortion that reduced the symmetry of the molecule to C_s. This suggested that lowering the symmetry to C_s might produce a one-dimensional 180° blade rotation TS. The appropriate desymmetrization of C_{2v}-**1**, followed geometry optimizations and frequency calculations at both levels, did indeed yield C_s-symmetric TS structures that possess only one imaginary normal mode (Table 1). Animation of this mode confirmed that C_s-**1** is a TS for 180° blade rotation at these levels of theory, and a stereoview of HF/STO-3G-optimized C_s-**1** is illustrated in Figure 1. Why might such a rotation proceed through a C_s-symmetric TS? Examination of the structure of C_s-**1** in Figure 1 shows that with mirror symmetry the two rings A on the rotating blade can be flattened against the bulk of the two perpendicular blades, thus minimizing the barrier to rotation. In this regard, the calculated free energies of C_s-**1** at the AM1 and HF/STO-3G levels are 21.5 and 27.2 kcal/mol, respectively, above those of D_3-**1** (see Table 1). These estimates of $\Delta G^{\ddagger}$ for the 180° blade rotation are a bit higher than the experimental value of 18.9 kcal/mol observed for a hexamethoxy derivative of **1**.[5]

It is worth noting that, for a molecule of the complexity of **1**, it is possible that more than one TS exists for the 180° blade rotation. Thus, there could conceivably be a C_2- or C_1-symmetric TS for this process that is lower in energy than C_s-**1**, but such a TS was not found. Another important feature of the C_s-symmetric 180° blade rotation TS structure is that, because of its mirror symmetry, this structure can evolve into either enantiomer of D_3-**1**, and thus 180° blade rotation provides an alternative path for the racemization of compound **1** (at least at these lower two levels of theory).

The process of 180° blade rotation is slightly more complex at the B3LYP/6-31G(d) level. Geometry optimization and frequency calculations for C_s-**1** at this level found this structure to be a saddle point of order 2. A further lowering of the symmetry is required to find a genuine TS, and for the first time the QST3 option in Gaussian 03 would have to be employed in order to locate the TS structure. (This algorithm requires initial and final structures and a TS guess structure, and the efficiency of the algorithm is strongly dependent on the quality of the guess.) Animation of the normal mode in C_s-**1** that does not correspond to the blade rotation suggested that a reasonable C_1-symmetric TS guess might be formed by bending the two vertical blades slightly in the same direction around the central ring. When such a distortion was applied, and the resulting structure employed as a TS guess for the QST3 option, no TS was found at the B3LYP/6-31G(d) level.

In such a situation, there are generally two ways to proceed. The first is to find a better force constant matrix for the optimization, and the second is to find a better TS guess structure. In this case, the program was first instructed to calculate the force constants at the HF/STO-3G level before beginning the TS search at the higher level, but this also failed to yield a transition state. For the next attempt, the same guess structure was employed for a TS search at the HF/3-21G level; and this calculation *did* yield a C_1-symmetric TS structure (verified by a frequency calculation). The HF/3-21G TS structure was now employed as a TS guess for a new B3LYP/6-31G(d) search, but once again no TS was found at this level. In near desperation, the HF/3-21G TS structure was used as the guess for a search at the HF/6-31G(d) level, in the hope that the incremental variation of the basis set, but not the method, would be successful. Fortunately, this approach yielded a C_1-symmetric TS structure, and the new HF/6-31G(d) TS was employed as the guess for yet another B3LYP/6-31G(d) TS search. This search finally gave the elusive TS, and the TS structure is illustrated in Figure 1. At the B3LYP/6-31G(d) level, the calculated free energy of the 180° blade rotation TS is 25.4 kcal/mol above the ground state, rather higher than the experimental value.

2.4. The ring C rotation transition state

The rotation of ring C is the only other conformational interconversion in compound **1** that might possess a symmetric TS structure. Using the QST3 option in Gaussian 03, the search was limited to structures with C_2 symmetry by choosing a C_2-symmetric TS guess. This was achieved simply by rotating one of the rings C of D_3-**1**. Starting from this guess, stationary points were located at all three levels of theory. At the AM1 and B3LYP/6-31G(d) levels, these C_2 structures are saddle points of order 2, but at the HF/STO-3G level, C_2-**1** is a one-dimensional TS, and this structure is illustrated in Figure 2. At the AM1 and B3LYP/6-31G(d) levels, the C_2 saddle points were desymmetrized, and the QST3 option was again used to locate the C_1-symmetric transition states for ring C rotation. Generally speaking, TS searches involving a simple process such as a phenyl rotation are much less difficult than ones involving large groups such as the blade rotation described in Section 2.3, and the ring C rotation TS searches converged without difficulty. The B3LYP/6-31G(d) ring C TS structure is also illustrated in Figure 2.

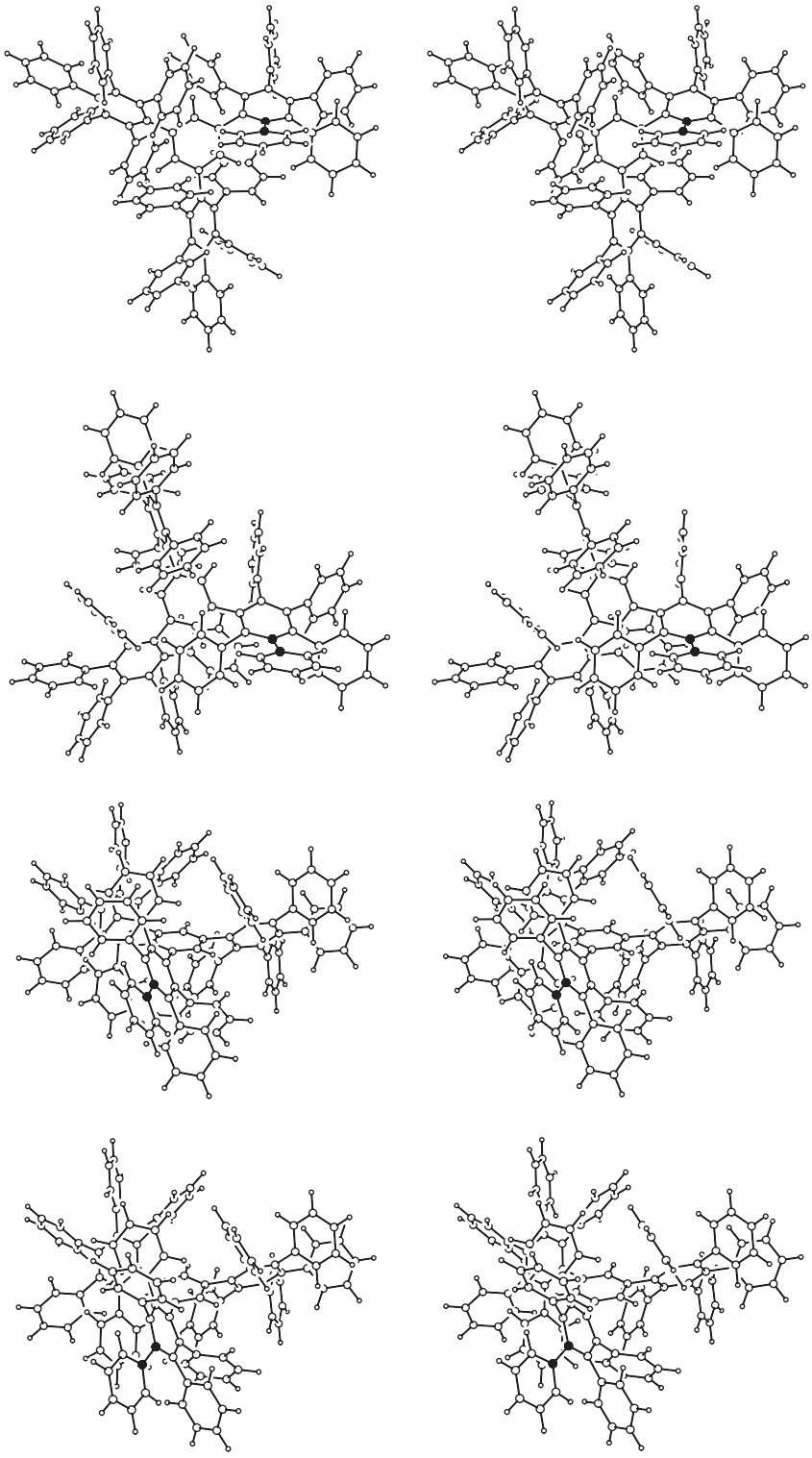

Figure 2. Stereoviews of calculated stationary point structures for compound **1**. Top to bottom: the B3LYP/6-31G(d) ring A rotation TS (C_1), the B3LYP/6-31G(d) ring B rotation TS (C_1), the HF/STO-3G ring C rotation TS (C_2), and the B3LYP/6-31G(d) ring C rotation TS (C_1). The solid black spheres are the carbon atoms around which the principal bond rotations occur.

The calculated free energies of the AM1, HF/STO-3G, and B3LYP/6-31G(d) transition states for ring C rotation are 19.1, 24.1, and 20.8 kcal/mol, respectively, above those for D_3-**1** (see Table 1). Unfortunately, there exists no experimental $\Delta G^{\ddagger}$ for this process for comparison.

2.5. The ring A and ring B rotation transition states

The C_1-symmetric transition states for the ring A and ring B rotations were located without difficulty by using the QST3 option in Gaussian 03, and frequency calculations on these

TS structures yielded one imaginary frequency for each, as expected (see Table 1). Stereoviews of both B3LYP/6-31G(d)-optimized rotational transition states are illustrated in Figure 2. As with the rotation of ring C, the ring A and ring B phenyl rotations have only limited effects on the structure of compound **1** in parts of the molecule remote from the rotating groups.

The free energies of the ring A rotation transition states at the AM1, HF/STO-3G, and B3LYP/6-31G(d) levels were 16.7, 25.8, and 19.9 kcal/mol above the ground state, the first comparing most favorably with the experimental $\Delta G^{\ddagger}$ of 16.9 kcal/mol.[4] Similarly, the free energies for the ring B rotation transition states were 19.0, 26.3, and 20.2 kcal/mol above the respective ground states at the three levels of theory, and once again the AM1 estimate was nearest to the experimental $\Delta G^{\ddagger}$ of 18.0 kcal/mol.[4]

2.6. Chromatographic resolution of compound 1

The computational results at all three levels of theory suggest that racemization of compound **1** most likely proceeds through triple 60° blade rotation, and the calculated barriers for this process are high enough (19–24 kcal/mol) to permit the resolution of **1** into its enantiomers, if not at room temperature, then at temperatures only slightly below. We have often employed chromatography on chiral media to resolve complex aromatic compounds,[13–15] and this seemed to be the simplest approach for the resolution of compound **1**. The results are illustrated in Figure 3.

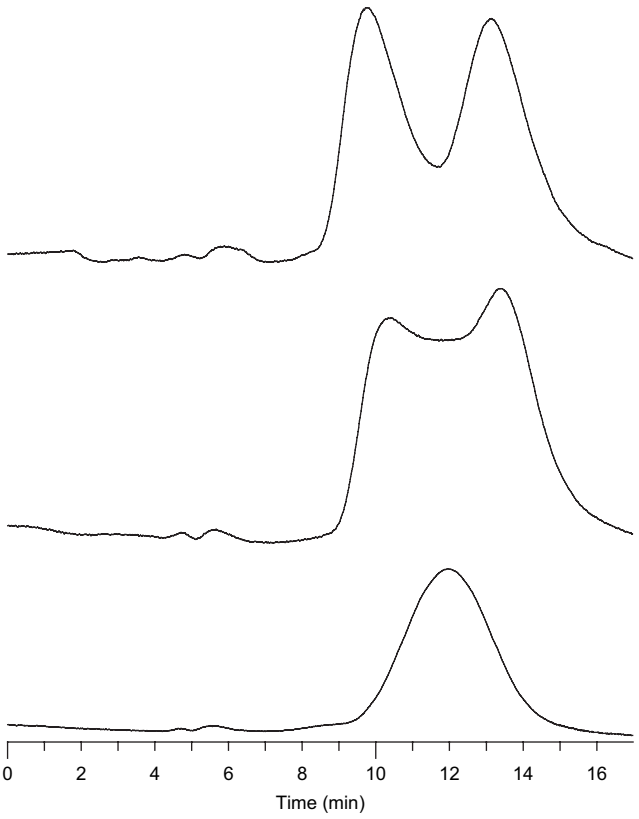

Figure 3. Chromatographic resolution of compound **1** at 5 °C (top), 15 °C (middle), and 22 °C (bottom). A Chiralcel OD column (25×0.46 cm) was employed; the compounds were eluted with ethanol (1 mL/min) with detection at 254 nm.

When chromatographed on a Chiralcel OD analytical column in ethanol at room temperature, compound **1** eluted as a single broad peak. However, at 15 °C, the chromatogram showed the characteristic profile of two slowly interconverting enantiomers, and at 5 °C, nearly complete resolution was observed. The resolution did not improve at lower temperatures. This is a favorable situation for the determination of enantiomerization rate constants by dynamic chromatography, and by using the method of Trapp,[16] k_{288K} was found to be 5.04×10^{-4} s^{-1}. From the Eyring equation, and assuming a transmission coefficient of 0.5, $\Delta G^{\ddagger}_{rac}$ is 20.8 kcal/mol at 15 °C.

3. Discussion

3.1. Ring rotation transition states

The A, B, and C ring rotations in compound **1** are not likely to be greatly different from those in simple hexaphenylbenzene derivatives, for which the experimentally determined barriers are 17–18 kcal/mol.[17,18] It is true that buttressing effects from large remote groups in hexaphenylbenzenes can raise the barriers slightly, but the effect is small.[19] For comparison with the present data, the TS for phenyl rotation in hexaphenylbenzene were located at the AM1, HF/STO-3G, and B3LYP/6-31G(d) levels of theory (data not shown). At all three levels, the TS structures possess C_s symmetry and strongly resemble the ring rotation TS structures illustrated in Figure 2 for compound **1**, in which the rotating rings are bent out of the planes of the central rings. The calculated ΔG's relative to hexaphenylbenzene's D_6 ground state were 19.8, 21.7, and 17.4 kcal/mol; thus the B3LYP value is in best agreement with the experimental data for these simple molecules.

This was not the case for compound **1**. For both the ring A and ring B rotations, the AM1-calculated barriers (16.7 and 19.0 kcal/mol, respectively) were in excellent agreement with the experimental values (16.9 and 18.0 kcal/mol,[4] respectively), but the B3LYP barriers were 2–3 kcal/mol too high and the HF/STO-3G barriers an unacceptable 8–9 kcal/mol too high. The poor performance of the HF/STO-3G method is perhaps not surprising; it frequently gives anomalous energies for aromatic compounds.[20] However, it is less obvious that the B3LYP estimate should become poorer as the molecule gets larger; after all, the same types of bonding and nonbonded interactions are present. A possible explanation lies in the fact that B3LYP/6-31G(d) calculations (and DFT methods in general) slightly overestimate bond distances in unsaturated hydrocarbons.[21–24] In small molecules this is a trivial effect, but in larger molecules the accumulation of these systematic errors can result in calculated molecular geometries that are significantly expanded when compared to experimental structures,[23,24] perhaps leading to significant errors in the energies.

3.2. Blade rotation transition states and implications for the mechanism of racemization

The calculated blade rotation TS structures are much more interesting than those for simple phenyl rotations, because

the geometry of a large molecule such as **1** can respond in unexpected ways to the motion of a large functional group. On the one hand, the TS structure for the triple 60° blade rotation (Fig. 1) retains very high symmetry (C_{3h}) and is probably not too far from the structure that a chemist might guess is the transition state for such a process. On the other hand, the 180° blade rotation TS structures (Fig. 1) are of low symmetry and exhibit large distortions in directions not obviously related to the motion of the rotating group. In all of these structures, but most especially in the B3LYP/6-31G(d) TS, the central ring of the rotating blade is bent into a boat conformation. This apparently allows the phenyl groups *ortho* to the bond around which rotation occurs (marked as solid spheres in Fig. 1) to bend as far away as possible from the other two, non-rotating blades. Interestingly, a very similar distortion of a pentaphenylphenyl blade is observed in the crystal structure (and presumed ground state) of decaphenylbiphenyl.[25,26]

The triple 60° blade rotation is the most likely process that interconverts the two enantiomers of compound **1** (Scheme 1). Compound **1** cannot be resolved into pure enantiomers at room temperature, but the resolution can be performed at low temperature. The experimental barrier for the racemization of compound **1**, $\Delta G^{\ddagger}_{rac}$=20.8 kcal/mol, was determined by dynamic chromatography[16] of **1** on a chiral support. The computational barrier was also found to be 20.8 kcal/mol at the B3LYP/6-31G(d) level, a perfect agreement. The AM1 barrier was 2 kcal/mol too low, and the HF/STO-3G TS was not located, but must be at least 3 kcal/mol too high if it proceeds, as is likely, through a C_{3h}-symmetric intermediate.

At first glance the theory and experiment would be appear to be in harmony, but a possible problem arises when one considers the 180° blade rotation TS. At the B3LYP/6-31G(d) level, the TS structure for this process has C_1 symmetry and does not interconvert enantiomers, but at the lower AM1 and HF/STO-3G levels, the TS structure has C_s symmetry, and thus 180° blade rotation represents an alternative pathway for racemization of **1**. In the 'computational world' this is not a problem, because, at every level of theory, the 180° blade rotation is a higher energy process than triple 60° blade rotation. However, the *experimental* barrier for 180° blade rotation is only 18.9 kcal/mol,[5] some 2 kcal/mol lower than the *experimental* barrier for enantiomerization. These results suggest that racemization does not occur via 180° blade rotation, and thus the TS for this process cannot have C_s symmetry. For this reason, the B3LYP/6-31G(d) TS structure is more likely to resemble the true TS, even though the B3LYP estimate of the 180° blade rotation barrier is too high.

3.3. The 'appropriate' computational level

Previous computational studies of molecular motion in complex polyphenylenes have chiefly employed empirical force fields in molecular dynamics simulations, sometimes supplemented with semiempirical calculations.[2a,c,f] We are unaware of any studies of the conformational reactions of these large molecules that employ ab initio or density functional calculations, and there are certainly none that fully characterize transition state structures for such conformational interconversions. On the other hand, the use of density functional methods for such work may be 'killing flies with sledgehammers'. In this study, each of the low-symmetry B3LYP/6-31G(d) frequency calculations required three weeks on our fastest computer! Was it worth it?

In fact, when one compares the calculated and experimental free energies of activation for the four processes for, which both values are available, the semiempirical AM1 method gave the best performance. The average deviation of its calculated barriers was only 0.4 kcal/mol from the experimental $\Delta G^{\ddagger}$'s, with a maximum deviation of only 2.6 kcal/mol. In contrast, the HF/STO-3G method gave barriers that were much too high, averaging 7 kcal/mol above the experimental values. The accuracy of the B3LYP/6-31G(d) barriers was significantly better, but these barriers still averaged 3 kcal/mol higher than experiment.

Because there is no unusual bonding in these structures, there is every reason to expect that a well-calibrated semiempirical method should do well. Given that the B3LYP calculations required approximately 500 times the computational resources to carry out as the AM1 calculations, there is no good reason to recommend the higher level of theory. Indeed, because all three methods employed here are calculations in the gas-phase, it is unlikely that any level of theory will give perfect correspondence with experimental measurements in solution. In order to reduce the errors to less than 1 kcal/mol (an impressive feat!), it will undoubtedly be necessary to include the solvent explicitly.

Nevertheless, there are valuable elements in the quantum calculations reported here. Chief among them is that they permit the viewing of the structures of *bona fide* computational transition states, giving the researcher a better idea of the degree of flexibility in these complex molecules, and the unusual motions and distortions required for processes casually described as 'functional group rotations'. Moreover, the general similarity of the B3LYP TS structures, so painfully obtained, to those derived at lower levels of theory, gives one confidence that these calculated transition states are reasonable, if still imperfect, descriptions of the conformational reactions.

Acknowledgements

This work was supported by National Science Foundation Grant CHE-0614879, and it is gratefully acknowledged.

Supplementary data

A PDF file containing a table of the calculated absolute energies (E), zero-point corrected energies (E+ZPE), and free energies (G_{298}) at the three levels of theory employed in this study, a PDF file containing larger, mono (non-stereo) drawings of the transition state structures in Figures 1 and 2, and an ASCII text file containing the atomic coordinates of the ground state and transition state structures calculated at the B3LYP/6-31G(d) level. Supplementary data associated with this article can be found in the online version, at doi:10.1016/j.tet.2007.09.021.

References and notes

1. (a) Berresheim, A. J.; Müller, M.; Müllen, K. *Chem. Rev.* **1999**, *99*, 1747–1785; (b) Watson, M. D.; Fechtenkötter, A.; Müllen, K. *Chem. Rev.* **2001**, *101*, 1267–1300; (c) Grimsdale, A. C.; Müllen, K. *Angew. Chem., Int. Ed.* **2005**, *44*, 5592–5629.
2. (a) Brocorens, P.; Zojer, E.; Comil, J.; Shuai, Z.; Leising, G.; Müllen, K.; Bredas, J. L. *Synth. Met.* **1999**, *100*, 141–162; (b) Wind, M.; Saalwächter, K.; Wiesler, U.-M.; Müllen, K.; Spiess, H. W. *Macromolecules* **2002**, *35*, 10071–10086; (c) Pricl, S.; Fermeglia, M.; Ferrone, M.; Asquini, A. *Carbon* **2003**, *41*, 2269–2283; (d) Marek, T.; Süvegh, K.; Vertes, A.; Ernst, A.; Bauer, R.; Weil, T.; Wiesler, U.; Klapper, M.; Müllen, K. *Radiat. Phys. Chem.* **2003**, *67*, 325–330; (e) Mondeshki, M.; Mihov, G.; Graf, R.; Spiess, H. W.; Müllen, K.; Papadopoulos, P.; Gitsas, A.; Floudas, G. *Macromolecules* **2006**, *39*, 9605–9613; (f) Carbone, P.; Calabretta, A.; Di Stefano, M.; Negri, F.; Müllen, K. *J. Phys. Chem. A* **2006**, *110*, 2214–2224.
3. Komber, H.; Stumpe, K.; Voit, B. *Macromol. Chem. Phys.* **2006**, *207*, 1814–1824.
4. Komber, H.; Stumpe, K.; Voit, B. *Tetrahedron Lett.* **2007**, *48*, 2655–2659.
5. Tong, L.; Ho, D. M.; Vogelaar, N. J.; Schutt, C. E.; Pascal, R. A., Jr. *J. Am. Chem. Soc.* **1997**, *119*, 7291–7302.
6. Frisch, M. J.; Trucks, G. W.; Schlegel, H. B.; Scuseria, G. E.; Robb, M. A.; Cheeseman, J. R.; Montgomery, J. A., Jr.; Vreven, T.; Kudin, K. N.; Burant, J. C.; Millam, J. M.; Iyengar, S. S.; Tomasi, J.; Barone, V.; Mennucci, B.; Cossi, M.; Scalmani, G.; Rega, N.; Petersson, G. A.; Nakatsuji, H.; Hada, M.; Ehara, M.; Toyota, K.; Fukuda, R.; Hasegawa, J.; Ishida, M.; Nakajima, T.; Honda, Y.; Kitao, O.; Nakai, H.; Klene, M.; Li, X.; Knox, J. E.; Hratchian, H. P.; Cross, J. B.; Bakken, V.; Adamo, C.; Jaramillo, J.; Gomperts, R.; Stratmann, R. E.; Yazyev, O.; Austin, A. J.; Cammi, R.; Pomelli, C.; Ochterski, J. W.; Ayala, P. Y.; Morokuma, K.; Voth, G. A.; Salvador, P.; Dannenberg, J. J.; Zakrzewski, V. G.; Dapprich, S.; Daniels, A. D.; Strain, M. C.; Farkas, O.; Malick, D. K.; Rabuck, A. D.; Raghavachari, K.; Foresman, J. B.; Ortiz, J. V.; Cui, Q.; Baboul, A. G.; Clifford, S.; Cioslowski, J.; Stefanov, B. B.; Liu, G.; Liashenko, A.; Piskorz, P.; Komaromi, I.; Martin, R. L.; Fox, D. J.; Keith, T.; Al-Laham, M. A.; Peng, C. Y.; Nanayakkara, A.; Challacombe, M.; Gill, P. M. W.; Johnson, B.; Chen, W.; Wong, M. W.; Gonzalez, C.; Pople, J. A. *Gaussian 03, Revision C.02*; Gaussian: Wallingford, CT, 2004.
7. Dewar, M. J. S.; Zoebisch, E. G.; Healy, E. F.; Stewart, J. J. P. *J. Am. Chem. Soc.* **1985**, *107*, 3902–3909.
8. Hehre, W. J.; Radom, L.; Schleyer, P. v. R.; Pople, J. A. *Ab Initio Molecular Orbital Theory*; John Wiley and Sons: New York, NY, 1986; pp 133–226.
9. Becke, A. D. *J. Chem. Phys.* **1993**, *98*, 5648–5652.
10. Lee, C.; Yang, W.; Parr, R. G. *Phys. Rev. B* **1988**, *37*, 785–789.
11. Clark, M.; Cramer, R. D., III; Van Opdenbosch, N. *J. Comput. Chem.* **1989**, *10*, 982–1012.
12. Halgren, T. A. J. *Comput. Chem.* **1996**, *17*, 490–519.
13. West, A. P., Jr.; Smyth, N.; Kraml, C. M.; Ho, D. M.; Pascal, R. A., Jr. *J. Org. Chem.* **1993**, *58*, 3502–3506.
14. Lu, J.; Ho, D. M.; Vogelaar, N. J.; Kraml, C. M.; Pascal, R. A., Jr. *J. Am. Chem. Soc.* **2004**, *126*, 11168–11169.
15. Lu, J.; Ho, D. M.; Vogelaar, N. J.; Kraml, C. M.; Bernhard, S.; Byrne, N.; Kim, L. R.; Pascal, R. A., Jr. *J. Am. Chem. Soc.* **2006**, *128*, 17043–17050.
16. Trapp, O. *Chirality* **2006**, *18*, 489–497.
17. Gust, D. *J. Am. Chem. Soc.* **1977**, *99*, 6980–6982.
18. Gust, D.; Patton, A. *J. Am. Chem. Soc.* **1978**, *100*, 8175–8181.
19. Patton, A.; Dirks, J. W.; Gust, D. *J. Org. Chem.* **1979**, *44*, 4749–4752.
20. For some examples, see: Zhang, J.; Ho, D. M.; Pascal, R. A., Jr. *J. Am. Chem. Soc.* **2001**, *123*, 10919–10926.
21. Martin, J. M. L.; El-Yazal, J.; Francois, J.-P. *Mol. Phys.* **1995**, *86*, 1437–1450.
22. Baldridge, K. K.; Siegel, J. S. *Angew. Chem., Int. Ed.* **1997**, *36*, 745–748.
23. Barnett, L.; Ho, D. M.; Baldridge, K. K.; Pascal, R. A., Jr. *J. Am. Chem. Soc.* **1999**, *121*, 727–733.
24. Pascal, R. A., Jr. *J. Phys. Chem. A* **2001**, *105*, 9040–9048.
25. Tong, L.; Lau, H.; Ho, D. M.; Pascal, R. A., Jr. *J. Am. Chem. Soc.* **1998**, *120*, 6000–6006.
26. Pascal, R. A., Jr.; Hayashi, N.; Ho, D. M. *Tetrahedron* **2001**, *57*, 3549–3555.